RESEARCH ARTICLE SUMMARY

AGING

Aging Fly Cell Atlas identifies exhaustive aging features at cellular resolution

Tzu-Chiao Lu†, Maria Brbić†, Ye-Jin Park, Tyler Jackson, Jiaye Chen, Sai Saroja Kolluru, Yanyan Qi, Nadja Sandra Katheder, Xiaoyu Tracy Cai, Seungjae Lee, Yen-Chung Chen, Niccole Auld, Chung-Yi Liang, Sophia H. Ding, Doug Welsch, Samuel D'Souza, Angela Oliveira Pisco, Robert C. Jones, Jure Leskovec, Eric C. Lai, Hugo J. Bellen, Liqun Luo, Heinrich Jasper*, Stephen R. Quake*, Hongjie Li*

INTRODUCTION: Aging is a natural process that is associated with the gradual decline of tissues in the body. This process increases the risk of developing various diseases, such as cardiovascular and neurodegenerative diseases and cancers. The study of aging has a long history, and several aging hypotheses have been proposed. Nonetheless, there are still many unanswered questions when it comes to understanding the effects of aging on the composition and maintenance of different cell types. It is also not clear whether all cell types age at the same rate or whether the transcriptome of one cell type can be used to predict age. Additionally, the genes and signaling pathways that contribute to aging in different cell types are not yet fully understood.

RATIONALE: *Drosophila melanogaster*, commonly known as the fruit fly, has played a vital role in advancing the fields of genetics, neurobiology, development, and aging. A large portion (~75%) of genes associated with human diseases have counterparts with functional similarity in the fly. The fly is also a useful model organism for studying the aging process, as it displays several age-related functional changes observed in humans, such as decreased motor activity, learning and memory, cardiac function, and fertility. Therefore, a comprehensive understanding of the molecular and genetic mechanisms underlying age-related decline in flies can provide valuable insights not only for aging studies in this species but also in other organisms, including humans.

RESULTS: Advancements in single-cell RNA sequencing technologies and the creation of the Fly Cell Atlas (FCA) have enabled the investigation of aging phenotypes at the single-cell level in *D. melanogaster*. Here, we present the Aging Fly Cell Atlas (AFCA), a single-nucleus transcriptomic map that characterizes changes in most tissues of male and female flies across their life span. Our analysis provides insights into age-related gene expression changes, alterations in cell composition, and common p[illegible] ways that correlate with aging. Notably, [illegible] observed an increase in fat body nuclei and elevated apoptotic markers in old indirect flight muscles, which potentially contribute to the age-related decrease in muscle nuclei. We also developed aging clock models that predict an animal's age from single-nucleus transcriptomic data. Additionally, we found variances in aging for expressed gene number and cell type identity, with different cell types being differentially affected by different aging features.

CONCLUSION: The AFCA is a valuable resource and will be of interest to the aging research community. It provides an important and timely resource for studying aging and age-related diseases. It has the potential to serve as a reference of whole-organism aging that can be used as a baseline for exploring different age-related diseases and understanding how different longevity perturbations increase life span at a cellular resolution. The ease of creating whole-fly aging atlases makes *D. melanogaster* a key model organism for examining the intersection of genetics, cell biology, and physiology going forward. We have developed a user-friendly data portal and provided access at the CELLxGENE. All resources can be accessed at https://hongjielilab.org/afca/. ■

The list of author affiliations is available in the full article online.
*Corresponding author. Email: jasperh@gene.com (H.J.); steve@quake-lab.org (S.R.Q.); hongjie.li@bcm.edu (H.L.)
†These authors contributed equally to this work.
Cite this article as T.-C. Lu *et al.*, *Science* **380**, eadg0934 (2023). DOI: 10.1126/science.adg0934

READ THE FULL ARTICLE AT
https://doi.org/10.1126/science.adg0934

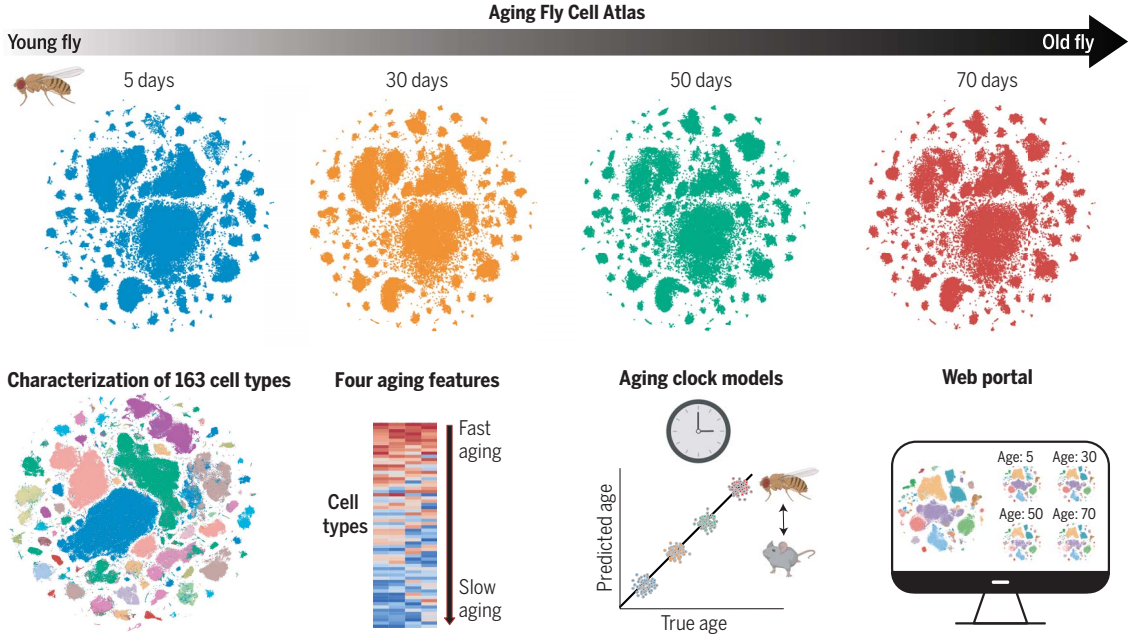

The Aging Fly Cell Atlas. The AFCA includes single-nucleus transcriptomes of 868,000 nuclei across the *Drosophila* life span. Males and females were sequenced separately. We characterized 163 distinct cell types, developed aging clock models, and combined four aging features to rank the aging rate of different cell types. [Figure created using Biorender]

RESEARCH ARTICLE

AGING

Aging Fly Cell Atlas identifies exhaustive aging features at cellular resolution

Tzu-Chiao Lu[1,2]†, Maria Brbić[3]†, Ye-Jin Park[1,2,4,5], Tyler Jackson[1,2,6], Jiaye Chen[1,2,7], Sai Saroja Kolluru[8,9,10], Yanyan Qi[1,2], Nadja Sandra Katheder[11], Xiaoyu Tracy Cai[11], Seungjae Lee[12], Yen-Chung Chen[13], Niccole Auld[1,2,6], Chung-Yi Liang[1,2,14], Sophia H. Ding[1,2], Doug Welsch[1,2], Samuel D'Souza[10], Angela Oliveira Pisco[10], Robert C. Jones[8], Jure Leskovec[15], Eric C. Lai[12], Hugo J. Bellen[2,4,5], Liqun Luo[16], Heinrich Jasper[11]*, Stephen R. Quake[8,9,10]*, Hongjie Li[1,2]*

Aging is characterized by a decline in tissue function, but the underlying changes at cellular resolution across the organism remain unclear. Here, we present the Aging Fly Cell Atlas, a single-nucleus transcriptomic map of the whole aging *Drosophila*. We characterized 163 distinct cell types and performed an in-depth analysis of changes in tissue cell composition, gene expression, and cell identities. We further developed aging clock models to predict fly age and show that ribosomal gene expression is a conserved predictive factor for age. Combining all aging features, we find distinctive cell type–specific aging patterns. This atlas provides a valuable resource for studying fundamental principles of aging in complex organisms.

Aging is characterized by the progressive decline in tissue function across the entire body. It is a major risk factor for a wide range of diseases, including cardiovascular diseases, cancers, and neurodegenerative diseases (*1*, *2*). Aging phenotypes have been observed and described for centuries, and a number of different aging hypotheses have been proposed (*3*). However, critical questions remain largely unaddressed in complex organisms: How does aging affect cell composition and the maintenance of specific cell types? Do different cell types age at the same rate? Can we use one cell type's transcriptome to predict age? What genes and signaling pathways drive aging in different cell types?

[1]Huffington Center on Aging, Baylor College of Medicine, Houston, TX 77030, USA. [2]Department of Molecular and Human Genetics, Baylor College of Medicine, Houston, TX 77030, USA. [3]School of Computer and Communication Sciences, Swiss Federal Institute of Technology (EPFL), CH-1015 Lausanne, Switzerland. [4]Program in Development, Disease Models and Therapeutics, Baylor College of Medicine, Houston, TX 77030, USA. [5]Jan and Dan Duncan Neurological Research Institute, Texas Children's Hospital, Houston, TX 77030, USA. [6]Program in Cancer Cell Biology, Baylor College of Medicine, Houston, TX 77030, USA. [7]Program in Quantitative and Computational Biosciences, Baylor College of Medicine, Houston, TX 77030, USA. [8]Department of Bioengineering, Stanford University, Stanford, CA 94305, USA. [9]Department of Applied Physics, Stanford University, Stanford, CA 94305, USA. [10]Chan Zuckerberg Biohub, San Francisco, CA 94158, USA. [11]Regenerative Medicine, Genentech, Inc., South San Francisco, CA 94080, USA. [12]Developmental Biology Program, Sloan Kettering Institute, New York, NY 10065, USA. [13]Department of Biology, New York University, New York, NY 10013, USA. [14]Institute of Biochemistry and Molecular Biology, National Yang Ming Chiao Tung University (NYCU), Taipei 112304, Taiwan. [15]Department of Computer Science, Stanford University, Stanford, CA 94305, USA. [16]Howard Hughes Medical Institute, Department of Biology, Stanford University, Stanford, CA 94305, USA.
***Corresponding author. Email: jasperh@gene.com (H.J.); steve@quake-lab.org (S.R.Q.); hongjie.li@bcm.edu (H.L.)**
†These authors contributed equally to this work.

The fruit fly, *Drosophila melanogaster*, has been at the basis of many key discoveries in genetics, neurobiology, development, and aging. About 75% of human disease–associated genes have functional homologs in the fly (*4*, *5*). Many of the age-related functional changes in humans are also observed in flies, including a decline in motor activity, learning and memory, cardiac function, and fertility (*6*). Hence, a proper description of the molecular and genetic basis of the age-related decline in flies should provide an important resource for aging studies not only in flies but also in other organisms.

The recent development of single-cell RNA sequencing (scRNA-seq) technologies and the establishment of the Fly Cell Atlas (FCA) (*7*), a single-nucleus transcriptomic atlas of *Drosophila* at the age of 5 days (5d hereafter), have made it possible to investigate aging phenotypes across the whole organism at single-cell resolution. Here, we present the Aging Fly Cell Atlas (AFCA), a single-nucleus transcriptomic map describing age-related changes in most tissues, including those that differ by sex. We performed an in-depth analysis of age-related gene expression and cell composition changes across the entire fly, as well as cell type–specific and common pathways that correlate with aging. Notably, we observed a significant increase of fat body nuclei and a drastic decrease in muscle nuclei with age. Furthermore, we developed aging clock models that predict the animal's biological age from the single-nucleus transcriptomic data. In addition, we found aging variances in expressed gene number and in cell type identity. Our analysis revealed that different cell types are differentially affected by different aging features. The AFCA provides a valuable resource for the *Drosophila* and aging communities as a reference to study aging and age-related diseases and to evaluate the success of antiaging regimens. We developed a website portal for data visualization and custom analyses and made data available at the CELLxGENE portal (figs. S1 and S2). All resources can be accessed at https://hongjielilab.org/afca.

Results

Single-nucleus transcriptomes of the entire fly at different ages

To generate the AFCA, we applied the same single-nucleus RNA sequencing (snRNA-seq) pipeline used for the FCA (5d adults) (*7*) and profiled the whole head and body at three additional ages (30d, 50d, and 70d). These time points were chosen to cover the life-span trajectory of a fly (Fig. 1A) and beyond, up to 70d, the estimated equivalent of 80- to 90-year-old humans. Male and female flies were sequenced separately, allowing the investigation of sexual dimorphism during aging (Fig. 1B). To achieve the most reliable analyses of aging features, we performed preprocessing of this newly generated aging data similarly to that done on the young FCA data (fig. S1A). Consistent with a previous scRNA-seq study of the aging fly brain (*8*), we found that young and old cells have a similar distribution in the *t*-distributed stochastic neighbor embedding (tSNE) space, suggesting that the whole organism largely maintains its cell types during aging (Fig. 1C). Overall, we obtained >868,000 nuclei covering all 17 broad cell type classes (Fig. 1, D and E). The detected numbers of expressed genes and unique molecular identifiers (UMIs) were largely consistent across different ages (fig. S3). The most abundant cell classes were neurons, epithelial cells, muscle cells, and fat cells. Next, we annotated those broad cell classes into detailed cell types.

AFCA cell type annotation and resource for studying cell type–specific aging

Because cell type–specific aging analysis largely depends on accurate cell type annotation, we took multiple approaches to ensure that our AFCA data were annotated with high confidence. We first co-clustered our aging data with the annotated FCA data, either from the head or body or from individual tissues. Then we transferred AFCA annotations using both a cluster-centered method and a supervised machine learning–based method (figs. S4 and S5). Overall, we found that these two approaches agree well, with ~80% overlap (Fig. 2A). The discrepancies of the nonoverlapping annotations were mostly due to uncharacterized cell types in the FCA data or cell types with aging differences. Next, we manually validated each annotation using cell type–specific markers. Marker validation confirmed the accuracy of our automatic annotation procedure, with a few exceptions, such as indirect flight muscles because of age-related loss of specific markers

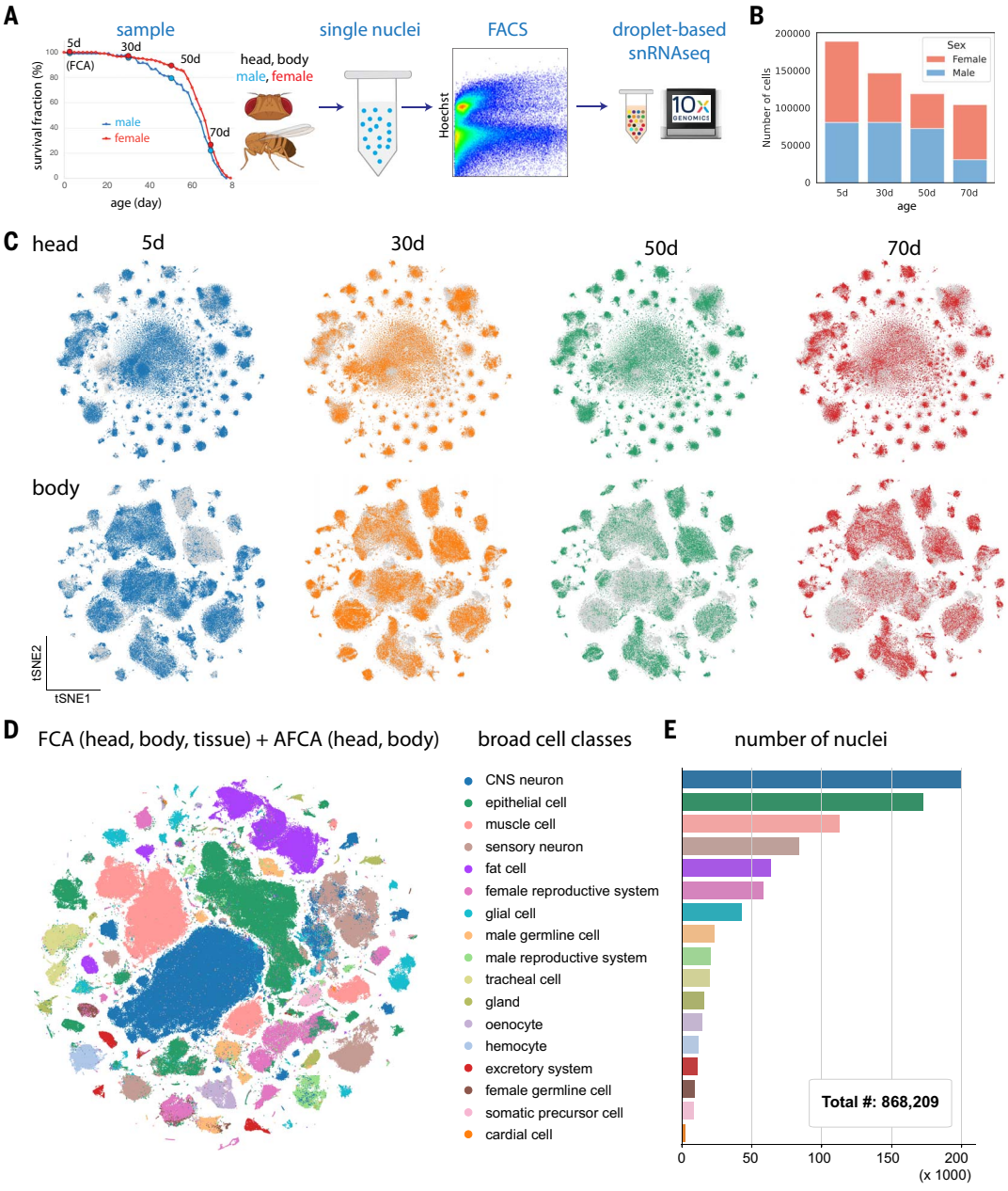

Fig. 1. Overview of the AFCA. (**A**) Flowchart of the snRNA-seq experiment. Flies were collected at 30, 50, and 70 days. The heads and bodies of males and females were processed separately. 5d samples were from the FCA. FACS, fluorescence-activated cell sorting. (**B**) Number of nuclei collected from different ages and sexes. (**C**) tSNE visualizations of the head and body samples from different ages. (**D**) tSNE visualizations showing broad cell classes of datasets integrated across different time points. (**E**) Number of nuclei for each broad cell class shown in (D).

(fig. S6, A and B) and gut cell types because of the high similarity between intestinal stem cells and renal stem cells (fig. S6C). These cell types were then manually added and corrected (figs. S5 and S7). Overall, we characterized 163 distinct cell types, including 91 cell types from the aging head and 72 cell types from the aging body (Fig. 2B and figs. S8 and S9).

For complex tissues such as the brain, more cell types can emerge when substantially more cells are sequenced (*9*–*11*). Indeed, 17 additional neuronal cell types emerged after combining young and old head data (Fig. 2C). Among them, four types are GABAergic neurons (*Gad1*+), two are glutamatergic neurons (*VGlut*+), and the remaining 11 are cholinergic neurons (*VAChT*+) (fig. S10).

Next, we assessed the reliability of AFCA data for investigating age-related changes in specific cell types. As a case study, we focused on the fly gut, for which the somatic stem cell lineage and its aging have been well characterized (*12*). In a healthy young fly gut, intestinal stem cells (ISCs) maintain gut homeostasis through proper proliferation and differentiation. In old flies, ISCs exhibit a high proliferation rate, and their daughter cells, enteroblasts (EBs), do not properly differentiate into mature enterocytes, leading to a dysplasia phenotype (*13*–*15*). We first extracted six major gut cell types and performed pseudotime trajectory analysis (*16*, *17*). There was a significant increase of ISCs and EBs along with a decrease of fully differentiated enterocytes, consistent with previous in vivo studies (Fig. 2D and fig. S11) (*18*), and we could identify genes that showed different dynamic patterns between young and old flies (fig. S11E). As demonstrated by this case study, the detailed annotations in our AFCA data offer a valuable resource to explore cell type– and tissue-specific aging signatures.

Cell composition changes during aging

In complex organisms, aging can affect cellular composition in different ways, such as changing stem cell proliferation or differentiation processes, altering cell identity, or inducing cell death. We assessed whether and how aging affects cellular composition across the whole fly. Note that our measurements are based on nuclei composition. Given that the

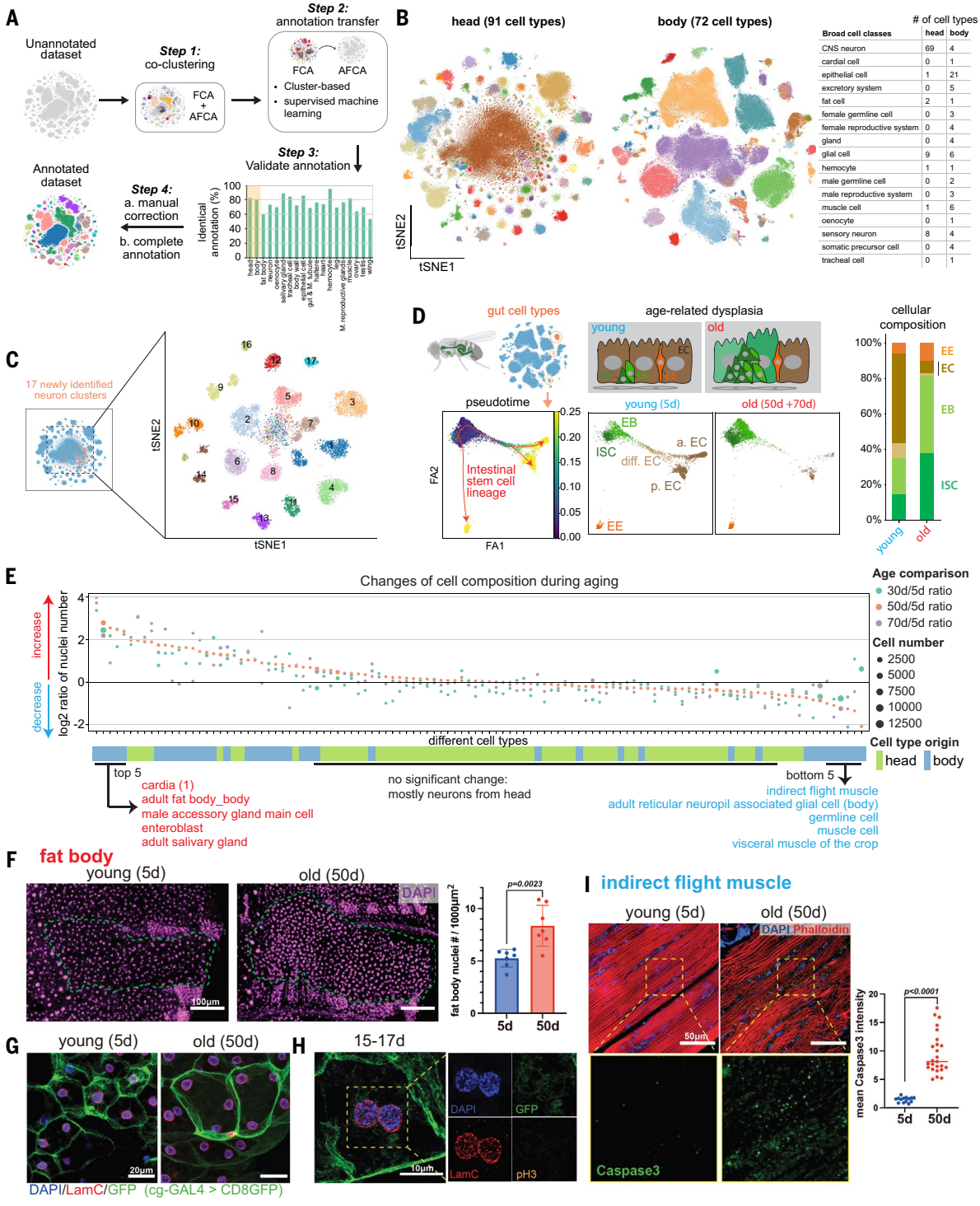

Fig. 2. AFCA resource and changes of cell composition during aging. (**A**) Flowchart of transferring annotations from the FCA to the AFCA. (**B**) Cell types annotated in the AFCA head and body shown on tSNE. The number of annotated cell types corresponding to the broad cell classes is shown in the table. (**C**) Identification of 17 additional neuronal clusters after combining AFCA and FCA head data. (**D**) Pseudotime and cellular composition of ISC and ISC-differentiated cell types. ISC, intestinal stem cell; EB, enteroblast; EC, enterocyte; EE, enteroendocrine cell; a. EC, anterior EC; p. EC, posterior EC; diff. EC, differentiating EC. (**E**) Changes of cellular composition during aging. Each dot represents one cell type. Each color compares one aged sample and the 5d sample. Dot sizes reflect the nuclear numbers of the corresponding cell type from the aged population. Tissue origins are indicated. (**F**) Comparison of the number of nuclei of the fat body from young and old flies. Nuclei are stained by 4′,6-diamidino-2-phenylindole (DAPI) and counted in each fly. The nuclear number is significantly increased in the 50d population (*t*-test, 50d versus 5d, $P = 0.0023$). Error bar, standard deviation (SD). (**G**) Representative confocal images showing nuclei in young and old fat body cells. The membrane is labeled by *cg-GAL4 > UAS-CD8GFP*. Nuclei are stained by DAPI and the LamC antibody. (**H**) Fat body cells with segregating nuclei stained by pH3, DAPI, LamC, and GFP. (**I**) Indirect flight muscle stained with cleaved-Caspase3 antibody, DAPI, and phalloidin. Cleaved-Caspase3 signals are significantly increased in the aged population (*t*-test, 50d versus 5d, $P < 0.0001$). Median numbers are indicated.

nuclei are extracted from the whole head and body with minimal sampling bias, the ratio for each cell type in our sequencing data should largely reflect their composition in vivo.

To perform reliable analyses, we focused on cell types that have >500 nuclei in total (112 cell types after filtering). We then calculated the composition changes by comparing three older ages (30d, 50d, and 70d) to young flies (5d). The top five increased cell types are cardia cells (proventriculus from the gut), fat body cells, male accessory gland main cells, EBs, and adult salivary gland cells (Fig. 2E). Comparing two consecutive ages showed similar results (fig. S12). Age-related increases of proventriculus cells, male accessory gland main cells, and EBs have been reported previously (*19*–*21*), confirming the quality of our data and analysis. Fat body cells are one of the most abundant cell types in *Drosophila*. They are polyploid, filled with lipid droplets, and tightly attached to the abdominal cuticle. These features make it difficult to isolate them or to compare their compositions using traditional methods. To our knowledge, an increase of fat body nuclei in old flies has not been reported. We were able to validate this observation (Fig. 2F).

Fat body cells are postmitotic cells, and no adult stem cells or progenitors have been reported for regeneration (*22*). To examine why fat body nuclei were increased in old flies, we first checked the number of nuclei within single cells using a fat body–specific GAL4 driving cell membrane green fluorescent protein (GFP). Many aged fat body cells exhibited an increase in cell size and contained multiple nuclei per cell (Fig. 2G). The multinucleated phenotype can potentially be caused by cell membrane fusion, as reported in other cell types (*23*), but it cannot explain the increase in the number of nuclei (Fig. 2, E and F). It has been reported that polyploid enterocytes from the fly gut can undergo nuclear cleavage without mitosis (a process called amitosis) (*24*). To test this possibility, we performed immunohistochemistry to detect the nuclear lamina protein, Lamin C (LamC), and a mitosis marker, Phospho-Histone H3 (pH3). We did not detect any mitotic events from >60 flies across different ages, but we did observe many cases where two nuclei were localized very close to each other and were negative for the mitotic marker (Fig. 2H). Three-dimensional reconstruction of confocal images confirmed that these nuclei were present in the same cell without a separating cell membrane (movies S1 to S3). Such events were captured across different ages (fig. S13). Together, these data suggest that fat body cells undergo nuclear division without cytokinesis across different ages, leading to multinucleated cells and an increase in the number of nuclei in older flies.

Among the top five decreased cell types are three types of muscle—indirect flight muscle, visceral muscle, and other muscle cells (mostly skeletal muscle) (Fig. 2E). Loss of muscle mass and strength, known as sarcopenia, is a conserved aging phenotype across different mammals, including humans (*25*). Our in vivo staining data confirmed the age-related degeneration of indirect flight muscles as well as a significant increase of an apoptosis marker, Caspase3, in old flies (Fig. 2I and fig. S14), consistent with a previous study (*26*). Germline cells also showed a significant decrease (Fig. 2E and fig. S12), presumably contributing to the decline of fecundity in old flies. Most cell types from the head, mostly neurons, showed minimal cellular composition changes (Fig. 2E and fig. S12).

Differentially expressed genes

Altered gene expression is another consequence of aging (*27*). To assess such changes, we performed differentially expressed gene (DEG) analysis between young and old flies and ranked cell types on the basis of the number of DEGs (Fig. 3A and fig. S15A). Again, we focused on 112 cell types with >500 cells for a reliable analysis. In the body, the cell type with the highest number of DEGs was the fat body, while the most affected cell type in the head was the outer photoreceptor (Fig. 3A).

To explore the dynamics of cell type–specific changes, we further examined the time window during which cell types change the most by computing DEG numbers between two neighboring ages (fig. S15B) and normalizing their ratios (Fig. 3B and fig. S16). This analysis revealed several notable insights (Fig. 3, B and C). Specifically, ~80% of the cell types showed major changes (>50% of DEGs) during the first time window, suggesting that 30-day-old flies have captured a large portion of age-related gene changes. Some cell types, such as the male accessory gland, showed minimal changes in the last time window, indicating that these cell types reach their maximum transcriptomic changes around 50d. However, 5.3% of cell types, including intestinal stem cells and cardia cells, showed drastic changes (>50% of DEGs) in the last time window, suggesting that they age at a slower rate during the first 50d. Other cell types such as outer photoreceptors and fat body cells showed a steady change. Hence, this analysis indicates that different cell types age at different rates and exhibit distinctive patterns of gene expression changes. We compared DEGs from the AFCA with those from the aging fly brain study (*8*) and found that they are well correlated (fig. S17).

By integrating cellular composition changes and DEG analysis, we determined which cell types were affected by those two parameters (Fig. 3D). Significantly affected cell types ("outliers") fell into four categories: (i) cells showing changes for both, such as fat body cells from the body, pericerebral adult fat mass (fat cells from the head), and male accessory gland main cells; (ii) cells showing high DEGs but minimal composition changes, such as outer photoreceptors and cone cells, consistent with a previous study reporting that age-related fly visual decline is not attributable to the loss of photoreceptors (*28*); (iii) cells showing decreased nuclear number and a moderate number of DEGs, such as indirect flight muscles; and (iv) cells showing increased nuclear number but minimal DEGs, such as cardia cells.

Next, we performed sex-related analysis. We first observed that female marker yolk protein genes (*Yp1*, *Yp2*, and *Yp3*) showed a significant decrease during aging in most female cell types, while the male markers (*roX1* and *roX2*) maintained high expression levels in most male cells (fig. S18, A and B). In addition, some genes, such as *Lsd-2* and *CG45050*, showed different trends between males and females with age (fig. S18C), suggesting that aging affects male and female cells differently. It has been shown previously that different cell types exhibit different DEGs in males and females at a young age (*7*). We next checked how these numbers change during aging. Generally, if one cell type showed a high or low number of DEGs at a young age, it maintained that high or low number during aging (fig. S19A). However, some cell types showed age-specific sex differences. For example, three cell types from the head—pericerebral adult fat mass, skeletal muscle, and hemocyte—all showed few DEGs in young flies but many DEGs in old flies (fig. S19, B and C). In contrast, three glial populations showed a significant decrease of DEGs with age. We also checked how sex affects the DEG number and cell composition and found that these two features highly correlate between male and female flies (fig. S19, D to G).

Analysis of gene pathways

Next, we investigated which genes and pathways are enriched in DEGs. Gene ontology (GO) analysis was performed for both up- and down-regulated genes compared between the 50d and 5d dataset (fig. S20). Most GO terms were cell type–specific (fig. S20A); only 20% of GO terms were shared by more than five cell types for down-regulated genes and 40% for up-regulated genes. We found that one GO term from down-regulated genes, "cytoplasmic translation," was shared by almost all cell types (fig. S20C). Cytoplasmic translation refers to the ribosome-mediated process for protein synthesis. Many transcripts of genes encoding ribosomal proteins (RPs) were decreased across cell types, consistent with previous studies (*29*). There were no globally shared GO terms among the up-regulated genes (fig. S20B). Instead, shared terms were restricted to specific groups of cells, for example, signal transduction seen in neuronal types and protein phosphorylation enriched in different non-neuronal cells.

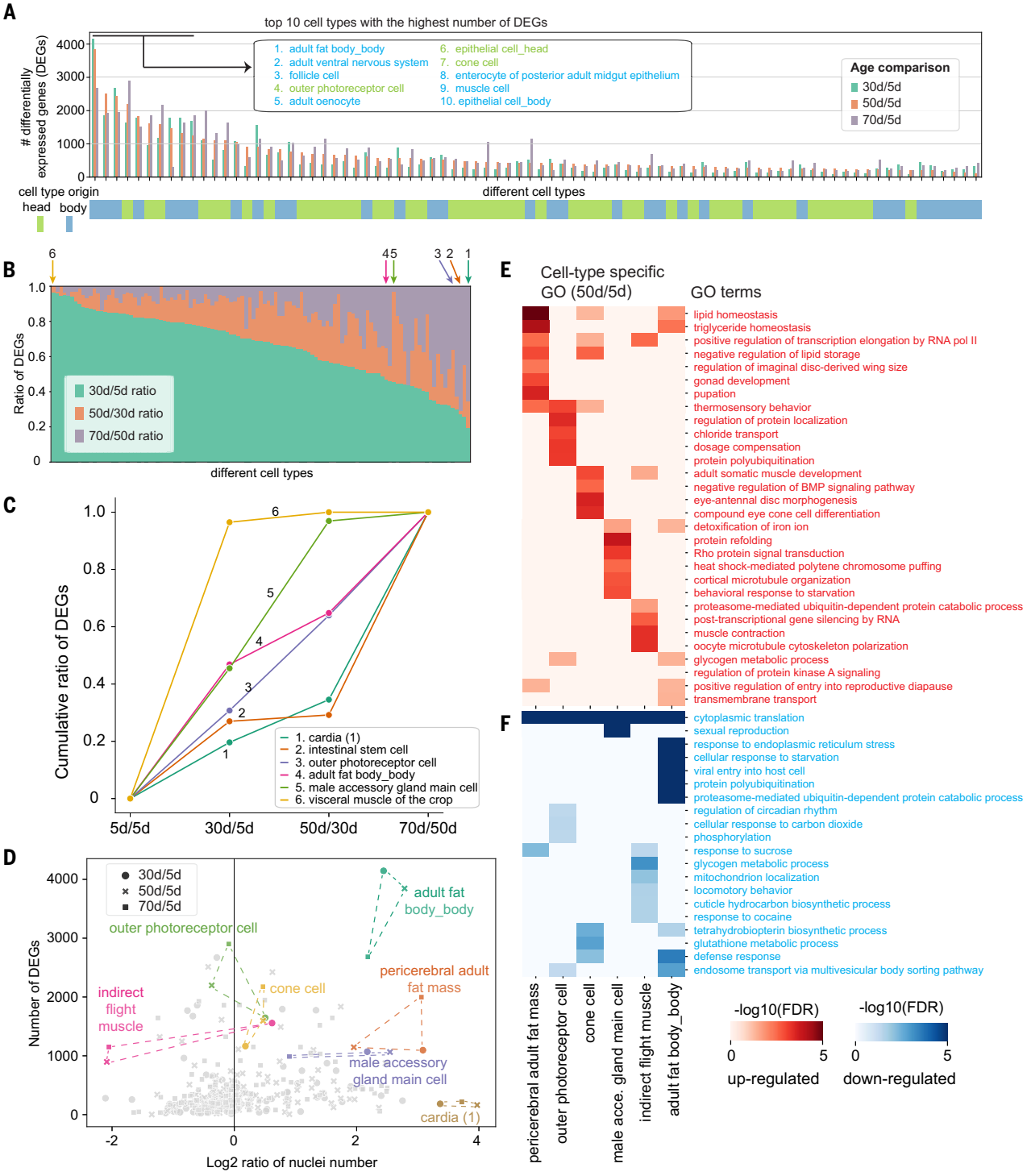

Fig. 3. Differentially expressed genes. (**A**) Number of DEGs from different cell types. Each age group is compared with the 5d population. Each line shows the number of DEGs from the indicated age comparison. Cell types are ranked by DEG numbers from high to low (50d versus 5d). The top 10 cell types are indicated. (**B**) Ratio of DEGs from each age comparison. Arrows point out representative cell types that are further compared in the next panel. (**C**) Cumulative ratios of DEGs from cell types indicated in (B). (**D**) Combination of DEG number and change of nuclear number illustrates different aging patterns. (**E** and **F**) Top five cell type–specific GO terms from selected cell types. (E) GO terms enriched in the selected cell types on the basis of up-regulated DEGs. (F) GO terms enriched in the selected cell types on the basis of down-regulated DEGs.

We next focused on GO terms enriched within a few cell types to understand the cell type–specific regulations (Fig. 3, E and F). Fat body cells from body and head (pericerebral adult fat mass) shared metabolic-related GO terms from up-regulated genes, such as lipid homeostasis and triglyceride homeostasis (Fig. 3E), reflecting common metabolic changes in these tissues. For indirect flight muscles, a reduction of locomotor behavior was observed and is likely to be caused by muscle degeneration (Fig. 3F) (*26*). Also, reproduction-related genes were strongly

decreased in male accessory gland main cells (Fig. 3F), consistent with the decline in reproductive ability in males (*30*). To summarize, we observed that genes involved in "cytoplasmic translation" are commonly decreased during aging in many cell types, whereas most other GO terms showed cell type–specific patterns.

Aging clock to predict the biological age

To predict the biological age of an animal or human, a number of different aging clock models have been recently developed using epigenetic markers and transcriptomic data (*8*, *31*, *32*). We investigated whether our snRNA-seq data can be used to develop aging clocks. To perform a more accurate prediction, we focused on cell types that have >200 cells at each age point (64 cell types). For each cell type, we trained a regression model (*33*) to predict age. We measured predictive performance using the coefficient of determination, R^2 (Fig. 4A). The average performance across all cell types was high (average R^2 = 0.79 for body and 0.84 for head; fig. S21).

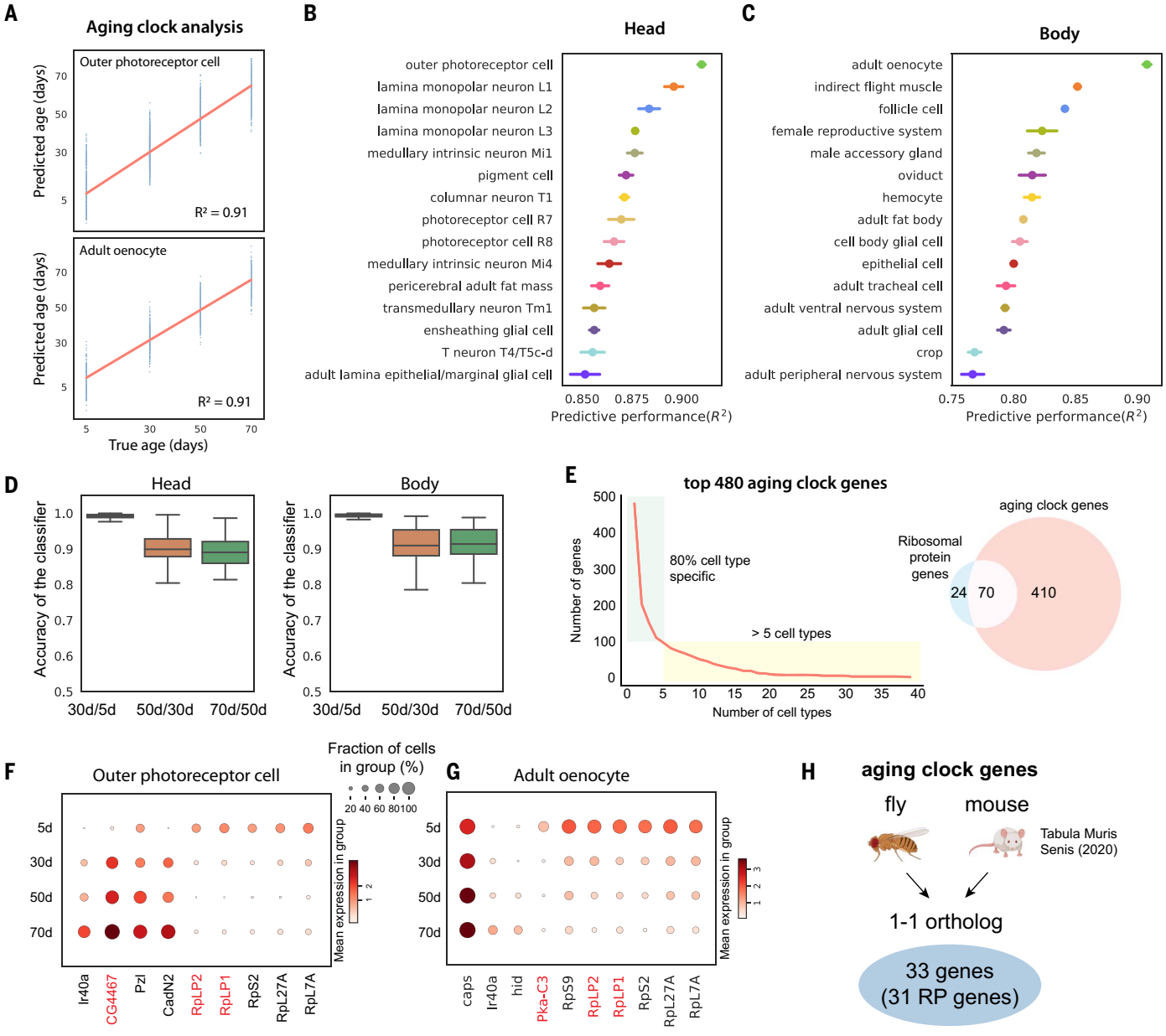

Fig. 4. Aging clock analysis. (**A**) Example of aging clocks for outer photoreceptor cells and adult oenocytes. The red line is the fitted regression line. Blue dots represent individual predictions wherein each dot corresponds to one cell. We measure performance as the proportion of the variance for an age variable that is explained by transcriptome (R^2). (**B** and **C**) Predictive performance of cell type–specific aging clocks for head and body cell types. Fifteen cell types with the highest scores are shown. Error bars are estimated as a SD over five runs. (**D**) Accuracy of logistic regression models trained to distinguish transcriptome between two consecutive time points. Boxplots show the distribution across head cell types (left) and body cell types (right). (**E**) Number of aging clock genes as a function of the number of cell types (left). Eighty percent of genes appear in fewer than five cell types. Out of 480 genes identified as aging clock genes, 70 encode RP genes (right). (**F** and **G**) Examples of aging clock genes for outer photoreceptor cell (F) and adult oenocyte (G). Cell type–specific genes that appear in fewer than five cell types are shown in black, while genes that appear in at least five cell types are shown in red. (**H**) Aging clock genes identified in flies and mice. Thirty-three genes are one-to-one orthologs between the two species, and 31 of these are RP genes.

Outer photoreceptor cells and oenocytes showed the highest predictive scores in head and body, respectively (Fig. 4, B and C). *Drosophila* oenocytes perform liver-like functions including lipid storage and metabolomics functions, similar to fat body cells, and also produce important cuticular pheromones (*34*). We confirmed that high scores were not caused by higher nuclear numbers (fig. S22A). We further asked whether there is a difference in predictive performance between different time windows and found that the largest transcriptomic differences are present between the first two ages (Fig. 4D).

Next, we focused on identifying aging clock genes that are used to predict the age. First, we found that most aging clock genes are used in a cell type–specific manner (Fig. 4E). We found that 70 out of 94 fly RP genes were identified as aging clock genes, showing age-related reductions in different cell types (Fig. 4, E to G). These data are consistent with our previous GO analysis where "cytoplasmic translation" is reduced in almost all cell types (fig. S20C). Decreased protein translation, which can be caused by the reduction of RPs, is a prevalent feature of aging (*35*). To determine what transcription factors might regulate the expression of RPs, we used the regulon information from the FCA (*7*, *36*) and identified several transcription factors regulating RP genes (fig. S23). Our data suggest that the reduction of ribosomal expression contributes to the age-related decrease of protein synthesis. To further investigate the relationship of aging clock genes across species, we identified aging clock genes from the Mouse Aging Cell Atlas (*27*). Among 33 overlapping aging clock genes from the fly and mouse, 31 genes encode RPs (Fig. 4H and figs. S24 and S25).

Comprehensive aging features

Through the above analyses, we noticed that different cell types are sensitive to different aging features. To gain a better understanding of cell type–specific aging, we investigated more aging features, including expressed gene number or transcript number (measured by UMI) changes and decline of cell identity (Fig. 5A).

Similar to the aging clock analysis, we only focused on cell types with at least 200 cells from each age. Gene and UMI numbers were previously found to decrease in the old fly brain (*8*). Consistent with previous observations, we observed decreases in gene and UMI number in central nervous system (CNS) neurons during aging (fig. S26A). To understand whether such a reduction is a general aging feature or not, we examined all other cell types. The overall trend of gene and UMI numbers was largely consistent (fig. S26B). We found that ~80% of cell types exhibited a decrease in expressed gene numbers, but 20% exhibited an increase, suggesting that aging affects expressed gene numbers in a cell type–specific manner (Fig. 5B). Head hemocytes and pericerebral adult fat mass had the greatest increase in expressed gene numbers, while oenocytes, ventral nervous system cells, and fat body cells had the greatest decrease (Fig. 5C and fig. S26C). We confirmed that this was not caused by sequencing depth (fig. S26D). Even though head and body fat body cells both increased in nuclear number (Fig. 3D), their expressed gene numbers showed the opposite trends.

Loss of cell type identity has been shown to occur during aging for certain cell types (*12*, *37*). However, how cell identity changes across the entire organism during aging remains uncharacterized. To assess whether established cellular gene expression programs that define cell identity change during aging, we developed a measurement to combine two ratios—loss of original markers and gain of new markers—by comparing old populations with young populations (Fig. 5D, left panel). We then ranked cell types by their cell identity decline score (Fig. 5D, right panel; fig. S27). The Neuroligin 1 gene, *Nlg1*, which was used as a marker gene to annotate the indirect flight muscle, showed a drastic decrease with age, as did a number of other young marker genes (Fig. 5D and fig. S6A). Meanwhile, many other gene transcripts, such as *Chchd2*, began to appear in this cell type with aging. Other than the indirect flight muscle, pericerebral adult fat mass and epithelial cells from the head were also found to exhibit a large decrease in cell type identity (fig. S28).

Correlation and ranking of aging features

We examined four different aging features: cell composition changes, DEGs, change of expressed gene numbers, and cell identity decline. To understand the overall correlation between them, we ranked each feature from the least age-related change to the most. After integrating four aging features, their correlations were compared using Spearman's correlation and clustered using the correlation scores (Fig. 5E). Among those features, DEG number and decline of cell identity were highly correlated, suggesting that cell types with large numbers of DEGs would usually fluctuate in the expression of marker genes. On the other hand, changes of nuclear number and expressed gene number were more correlated with each other.

Next, we summed different feature ranks and sorted cell types by the total rank sums, with a higher rank indicating a more "aged" cell type (Fig. 5F and fig. S29). Notably, the top three cell types include three adipose cell types—oenocytes, fat body cells, and pericerebral adult fat mass—suggesting that those cells age faster than other cell types. Following them in the ranking are male accessory gland main cells, indirect flight muscle, and enteroblasts. Generally, neurons and glia from the nervous system age slower than other cell types (Fig. 5F). In summary, our analysis provided the first exhaustive analysis of different aging features and revealed the aging rates of different cell types across the entire organism.

Discussion

The cell atlas approach is emerging as a powerful tool to systematically study aging in different organisms, including worms (*38*, *39*), mice (*27*), and humans (*40*). A recent study performed cross-species analysis with scRNA-seq data from three species, including *D. melanogaster* (*41*). Our AFCA provides a complementary dataset and thorough analyses for studying aging features across the whole organism.

One interesting observation is the increase of fat body nuclei during aging. *Drosophila* fat body is a liver-like tissue that stores fat and serves as a detoxifying and immune-responsive organ. Adult fat body cells are postmitotic polyploid cells without a stem cell or progenitor population (*22*). How do they increase their nuclear number? Our observations suggest that these polyploid cells increase their number of nuclei by nuclear cleavage without cytokinesis, forming multinucleated cells. To complete karyokinesis, the nuclear envelope needs to be reassembled or reorganized. Fat body cells have been shown to undergo a decrease in nuclear envelope integrity as a result of the loss of Lamin B during aging (*42*), suggesting that the loss of nuclear envelope integrity may be associated with the multinucleation phenomenon. On the other hand, multinucleated cells have also been observed in the fly male accessory gland (*43*, *44*) and subperineurial glial cells (*45*), suggesting that multinucleated cells play specific roles in *Drosophila*. Multinucleated cells have been observed in species other than *Drosophila*, including mushrooms (*46*), plants (*47*), and the liver cells of humans and mice (*48*, *49*). Understanding the formation and regulation of multinucleated cells in the aging organism may provide new insights into an evolutionarily conserved phenomenon, as well as into the potential roles of multinucleated cells in age-related diseases.

In this study, we focused on four different aging features. Although these features cover several key aspects of age-related changes, the picture is incomplete. Additional aging measurements may reveal more specific aging patterns. For example, we investigated the change of alternative polyadenylation (APA) patterns, which can reflect short or long 3′ untranslated region usage for different isoforms (*50*), and found that neuronal extended 3′ isoforms were progressively depleted during aging. This phenotype is more obvious at 70d and more pronounced in females than in males (fig. S30). These data imply a global change in posttranscriptional regulation in aging neurons. Thus, future analysis may help elucidate additional aging patterns.

One major goal of this study was to characterize how different cell types age across

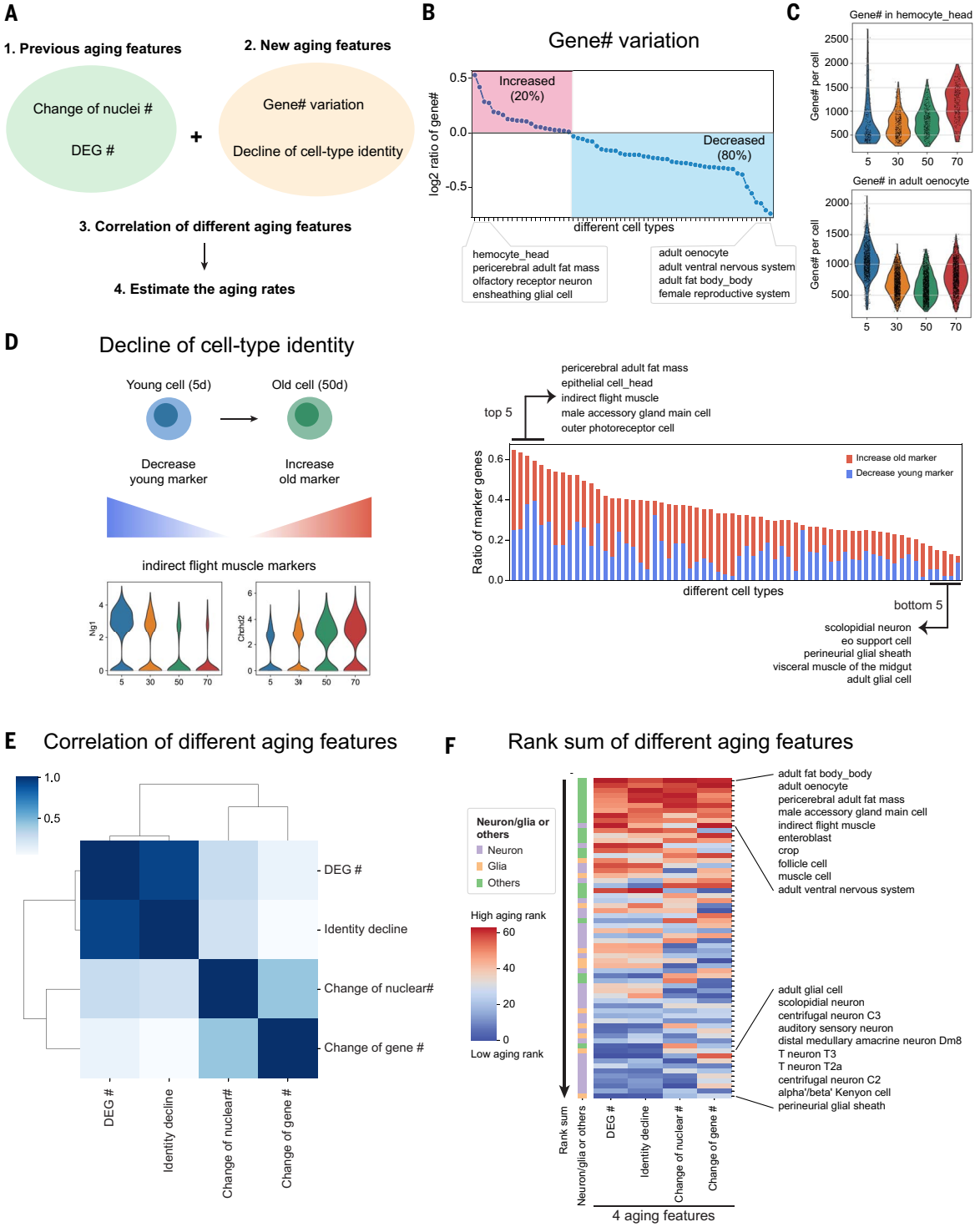

Fig. 5. Systematic comparisons of different aging features. (**A**) Flowchart for the comparison of different aging features. (**B**) Expressed gene numbers per cell from each cell type are compared between 50d and 5d flies. The red block shows cell types with increased expressed gene numbers, while the blue block includes cell types with decreased ones. (**C**) Two cell types, hemocyte from the head and oenocyte, have the highest increase and decrease, respectively, of expressed gene numbers per cell. (**D**) Decline of cell identity during aging. The left panel illustrates two different mechanisms of decreasing cell identity. The right panel shows the ratio of marker genes decreasing cell identity. Each line in the right panel represents one cell type. (**E**) Spearman's correlation of different aging features. (**F**) Rank sums of different aging features. The heatmap shows the overall rank sum scores from different cell types. High aging ranks are shown in red, while low aging ranks are shown in blue. Neuron- or glia-related cell types are indicated beside the heatmap.

the organism. Our analysis using different aging features provides several key insights. First, different cell types have distinct aging patterns. For example, the ventral nervous system showed high ranks for three aging features but a low rank for the change of nuclear number, while scolopidia neurons showed low ranks for three aging features but high ranks for the change in expressed gene number (Fig. 5F). This observation is not unexpected, considering that each cell type carries a specific function. Second, we observed a divergence in the contribution of individual cell types to a tissue's aging. For example, in the female reproductive system, follicle cells were ranked very high (eighth of 64 cell types), but germline cells were ranked near the bottom (41st of 64 cell types) (fig. S29A). This indicates that age-related declines of female fertility may be due to the aging of follicle cells. Third, the top-ranked cell types include all adipose cells. This is surprising, and we do not fully understand the underlying mechanisms. It may be linked to the fact that these cell types play multiple critical roles in different physiological conditions, such as lipid storage and metabolism,

immune responses, and interorgan communication with muscles and gut (*22*, *51*, *52*).

Materials and methods summary

This study involved collecting fly head and body samples from wild-type F1 flies from the cross between female W^{1118} and male Oregon R (OreR). Samples from different ages were dissected and stored at −80°C after flash-freezing with liquid nitrogen. The snRNA-seq was prepared using the FCA protocol (*7*), and each age group had 12 samples with six females and six males. The libraries were sequenced using NovaSeq 6000 (Illumina).

FASTQ files were filtered for index-hooping reads using 10x Genomics index-hopping-filter software. The Cell Ranger (version 4.0.0) index was built using the *D. melanogaster* genome (FlyBase r6.31) and the pre-mRNA GTF established by the FCA. Cell Ranger Count was used to estimate the nuclei number and gene expression from each nucleus. Nuclei from different sexes and ages of flies were integrated using Harmony, and cell type annotations from FCA samples were transferred to AFCA samples using a cluster-centered or machine learning–based method, followed by manual corrections.

For cell composition, age-specific ratios were obtained by dividing the number of nuclei in each cell type from one specific age by the total number of nuclei in the corresponding age. The relative ratios were then compared between the young (5d) and old populations. Wilcoxon rank sum tests were used to compare gene expression between different ages or sexes, and genes with a false discovery rate (FDR) of <0.05 were considered to be differentially expressed. The differential expression of the top 200 marker genes from 5d and 50d samples was used to estimate declines of cell type identity. Aging rates of each cell type were calculated by integrating different aging features and ranking the sums of aging ranks from high to low.

REFERENCES AND NOTES

1. C. López-Otín, M. A. Blasco, L. Partridge, M. Serrano, G. Kroemer, The hallmarks of aging. *Cell* **153**, 1194–1217 (2013). doi: 10.1016/j.cell.2013.05.039; pmid: 23746838
2. T. Niccoli, L. Partridge, Ageing as a risk factor for disease. *Curr. Biol.* **22**, R741–R752 (2012). doi: 10.1016/j.cub.2012.07.024; pmid: 22975005
3. D. Harman, The free radical theory of aging. *Antioxid. Redox Signal.* **5**, 557–561 (2003). doi: 10.1089/152308603770310202; pmid: 14580310
4. H. J. Bellen, C. Tong, H. Tsuda, 100 years of *Drosophila* research and its impact on vertebrate neuroscience: A history lesson for the future. *Nat. Rev. Neurosci.* **11**, 514–522 (2010). doi: 10.1038/nrn2839; pmid: 20383202
5. D. Baldridge *et al*., Model organisms contribute to diagnosis and discovery in the undiagnosed diseases network: Current state and a future vision. *Orphanet J. Rare Dis.* **16**, 206 (2021). doi: 10.1186/s13023-021-01839-9; pmid: 33962631
6. M. S. Grotewiel, I. Martin, P. Bhandari, E. Cook-Wiens, Functional senescence in *Drosophila melanogaster*. *Ageing Res. Rev.* **4**, 372–397 (2005). doi: 10.1016/j.arr.2005.04.001; pmid: 16024299
7. H. Li *et al*., Fly Cell Atlas: A single-nucleus transcriptomic atlas of the adult fruit fly. *Science* **375**, eabk2432 (2022). doi: 10.1126/science.abk2432; pmid: 35239393
8. K. Davie *et al*., A single-cell transcriptome atlas of the aging *Drosophila* brain. *Cell* **174**, 982–998.e20 (2018). doi: 10.1016/j.cell.2018.05.057; pmid: 29909982
9. J. Janssens *et al*., Decoding gene regulation in the fly brain. *Nature* **601**, 630–636 (2022). doi: 10.1038/s41586-021-04262-z; pmid: 34987221
10. H. Zeng, What is a cell type and how to define it? *Cell* **185**, 2739–2755 (2022). doi: 10.1016/j.cell.2022.06.031; pmid: 35868277
11. G. La Manno *et al*., Molecular architecture of the developing mouse brain. *Nature* **596**, 92–96 (2021). doi: 10.1038/s41586-021-03775-x; pmid: 34321664
12. H. Li, H. Jasper, Gastrointestinal stem cells in health and disease: From flies to humans. *Dis. Model. Mech.* **9**, 487–499 (2016). doi: 10.1242/dmm.024232; pmid: 27112333
13. H. Jasper, Intestinal stem cell aging: origins and interventions. *Annu. Rev. Physiol.* **82**, 203–226 (2020). doi: 10.1146/annurev-physiol-021119-034359; pmid: 31610128
14. C. A. Micchelli, N. Perrimon, Evidence that stem cells reside in the adult *Drosophila* midgut epithelium. *Nature* **439**, 475–479 (2006). doi: 10.1038/nature04371; pmid: 16340959
15. B. Ohlstein, A. Spradling, The adult *Drosophila* posterior midgut is maintained by pluripotent stem cells. *Nature* **439**, 470–474 (2006). doi: 10.1038/nature04333; pmid: 16340960
16. F. A. Wolf *et al*., PAGA: Graph abstraction reconciles clustering with trajectory inference through a topology preserving map of single cells. *Genome Biol.* **20**, 59 (2019). doi: 10.1186/s13059-019-1663-x; pmid: 30890159
17. M. Jacomy, T. Venturini, S. Heymann, M. Bastian, ForceAtlas2, a continuous graph layout algorithm for handy network visualization designed for the Gephi software. *PLOS ONE* **9**, e98679 (2014). doi: 10.1371/journal.pone.0098679; pmid: 24914678
18. I. A. Rodriguez-Fernandez, H. M. Tauc, H. Jasper, Hallmarks of aging *Drosophila* intestinal stem cells. *Mech. Ageing Dev.* **190**, 111285 (2020). doi: 10.1016/j.mad.2020.111285; pmid: 32544407
19. A. Rezaei, M. S. Krishna, H. T. Santhosh, Male age affects female mate preference, quantity of accessory gland proteins, and sperm traits and female fitness in *D. melanogaster*. *Zoolog. Sci.* **32**, 16–24 (2015). doi: 10.2108/zs140121; pmid: 25660692
20. B. Biteau, C. E. Hochmuth, H. Jasper, JNK activity in somatic stem cells causes loss of tissue homeostasis in the aging *Drosophila* gut. *Cell Stem Cell* **3**, 442–455 (2008). doi: 10.1016/j.stem.2008.07.024; pmid: 18940735
21. J. C. Regan *et al*., Sex difference in pathology of the ageing gut mediates the greater response of female lifespan to dietary restriction. *eLife* **5**, e10956 (2016). doi: 10.7554/eLife.10956; pmid: 26878754
22. E. L. Arrese, J. L. Soulages, Insect fat body: Energy, metabolism, and regulation. *Annu. Rev. Entomol.* **55**, 207–225 (2010). doi: 10.1146/annurev-ento-112408-085356; pmid: 19725772
23. V. P. Losick, D. T. Fox, A. C. Spradling, Polyploidization and cell fusion contribute to wound healing in the adult *Drosophila* epithelium. *Curr. Biol.* **23**, 2224–2232 (2013). doi: 10.1016/j.cub.2013.09.029; pmid: 24184101
24. E. M. Lucchetta, B. Ohlstein, Amitosis of polyploid cells regenerates functional stem cells in the *Drosophila* intestine. *Cell Stem Cell* **20**, 609–620.e6 (2017). doi: 10.1016/j.stem.2017.02.012; pmid: 28343984
25. T. J. Doherty, Invited review: Aging and sarcopenia. *J. Appl. Physiol.* **95**, 1717–1727 (2003). doi: 10.1152/japplphysiol.00347.2003; pmid: 12970377
26. H.-J. Jeon *et al*., Age-related change in γH2AX of *Drosophila* muscle: Its significance as a marker for muscle damage and longevity. *Biogerontology* **16**, 503–516 (2015). doi: 10.1007/s10522-015-9573-0; pmid: 25860864
27. Tabula Muris Consortium, A single-cell transcriptomic atlas characterizes ageing tissues in the mouse. *Nature* **583**, 590–595 (2020). doi: 10.1038/s41586-020-2496-1; pmid: 32669714
28. H. Hall *et al*., Transcriptome profiling of aging *Drosophila* photoreceptors reveals gene expression trends that correlate with visual senescence. *BMC Genomics* **18**, 894 (2017). doi: 10.1186/s12864-017-4304-3; pmid: 29162050
29. Y. Gonskikh, N. Polacek, Alterations of the translation apparatus during aging and stress response. *Mech. Ageing Dev.* **168**, 30–36 (2017). doi: 10.1016/j.mad.2017.04.003; pmid: 28414025
30. H. Ruhmann, M. Koppik, M. F. Wolfner, C. Fricke, The impact of ageing on male reproductive success in *Drosophila melanogaster*. *Exp. Gerontol.* **103**, 1–10 (2018). doi: 10.1016/j.exger.2017.12.013; pmid: 29258876
31. S. Horvath, K. Raj, DNA methylation-based biomarkers and the epigenetic clock theory of ageing. *Nat. Rev. Genet.* **19**, 371–384 (2018). doi: 10.1038/s41576-018-0004-3; pmid: 29643443
32. M. T. Buckley *et al*., Cell-type-specific aging clocks to quantify aging and rejuvenation in neurogenic regions of the brain. *Nat. Aging* **3**, 121–137 (2023). doi: 10.1038/s43587-022-00335-4; pmid: 37118510
33. H. Zou, T. Hastie, Regularization and variable selection via the elastic net. *J. R. Stat. Soc. Series B Stat. Methodol.* **67**, 301–320 (2005). doi: 10.1111/j.1467-9868.2005.00503.x
34. A. C. Ghosh *et al*., *Drosophila* PDGF/VEGF signaling from muscles to hepatocyte-like cells protects against obesity. *eLife* **9**, e56969 (2020). doi: 10.7554/eLife.56969; pmid: 33107824
35. N. Basisty, J. G. Meyer, B. Schilling, Protein turnover in aging and longevity. *Proteomics* **18**, e1700108 (2018). doi: 10.1002/pmic.201700108; pmid: 29453826
36. S. Aibar *et al*., SCENIC: Single-cell regulatory network inference and clustering. *Nat. Methods* **14**, 1083–1086 (2017). doi: 10.1038/nmeth.4463; pmid: 28991892
37. H. Izgi *et al*., Inter-tissue convergence of gene expression during ageing suggests age-related loss of tissue and cellular identity. *eLife* **11**, e68048 (2022). doi: 10.7554/eLife.68048; pmid: 35098922
38. S. M. Gao *et al*., Aging atlas reveals cell-type-specific regulation of pro-longevity strategies. bioRxiv 2023.02.28.530490 [Preprint] (2023). https://doi.org/10.1101/2023.02.28.530490.
39. A. E. Roux *et al*., The complete cell atlas of an aging multicellular organism. bioRxiv 2022.06.15.496201 [Preprint] (2022). https://doi.org/10.1101/2022.06.15.496201.
40. A. Sziraki *et al*., A global view of aging and Alzheimer's pathogenesis-associated cell population dynamics and molecular signatures in the human and mouse brains. bioRxiv 2022.09.28.509825 [Preprint] (2022). https://doi.org/10.1101/2022.09.28.509825.
41. R. Wang *et al*., Construction of a cross-species cell landscape at single-cell level. *Nucleic Acids Res.* **51**, 501–516 (2023). doi: 10.1093/nar/gkac633; pmid: 35929025
42. H. Chen, X. Zheng, Y. Zheng, Age-associated loss of lamin-B leads to systemic inflammation and gut hyperplasia. *Cell* **159**, 829–843 (2014). doi: 10.1016/j.cell.2014.10.028; pmid: 25417159
43. M. J. Bertram, G. A. Akerkar, R. L. Ard, C. Gonzalez, M. F. Wolfner, Cell type-specific gene expression in the *Drosophila melanogaster* male accessory gland. *Mech. Dev.* **38**, 33–40 (1992). doi: 10.1016/0925-4773(92)90036-J; pmid: 1525037
44. A. M. Box *et al*., Endocycles support tissue growth and regeneration of the adult *Drosophila* accessory gland. bioRxiv 719013 [Preprint] (2022). https://doi.org/10.1101/719013.
45. Y. Unhavaithaya, T. L. Orr-Weaver, Polyploidization of glia in neural development links tissue growth to blood-brain barrier integrity. *Genes Dev.* **26**, 31–36 (2012). doi: 10.1101/gad.177436.111; pmid: 22215808
46. T. Gehrmann *et al*., Nucleus-specific expression in the multinuclear mushroom-forming fungus *Agaricus bisporus* reveals different nuclear regulatory programs. *Proc. Natl. Acad. Sci. U.S.A.* **115**, 4429–4434 (2018). doi: 10.1073/pnas.1721381115; pmid: 29643074
47. P. von Aderkas, G. Rouault, R. Wagner, S. Chiwocha, A. Roques, Multinucleate storage cells in Douglas-fir (*Pseudotsuga menziesii* (Mirbel) Franco) and the effect of seed parasitism by the chalcid *Megastigmus spermotrophus* Wachtl. *Heredity* **94**, 616–622 (2005). doi: 10.1038/sj.hdy.6800670; pmid: 15829985
48. H.-Z. Chen *et al*., Canonical and atypical E2Fs regulate the mammalian endocycle. *Nat. Cell Biol.* **14**, 1192–1202 (2012). doi: 10.1038/ncb2595; pmid: 23064266
49. B. N. Kudryavtsev, M. V. Kudryavtseva, G. A. Sakuta, G. I. Stein, Human hepatocyte polyploidization kinetics in the course of life cycle. *Virchows Arch. B Cell Pathol. Incl. Mol. Pathol.* **64**, 387–393 (1993). doi: 10.1007/BF02915139; pmid: 8148960
50. S. Lee *et al*., Diverse cell-specific patterns of alternative polyadenylation in *Drosophila*. *Nat. Commun.* **13**, 5372 (2022). doi: 10.1038/s41467-022-32305-0; pmid: 36100597
51. X. Zhao, J. Karpac, Glutamate metabolism directs energetic trade-offs to shape host-pathogen susceptibility in *Drosophila*. *Cell Metab.* **33**, 2428–2444.e8 (2021). doi: 10.1016/j.cmet.2021.10.003; pmid: 34710355
52. N. Chatterjee, N. Perrimon, What fuels the fly: Energy metabolism in *Drosophila* and its application to the study of obesity and diabetes. *Sci. Adv.* **7**, eabg4336 (2021). doi: 10.1126/sciadv.abg4336; pmid: 34108216
53. T.-C. Lu, MeshifLu/AFCA: AFCA_v1.0 (AFCA_v1.0), Zenodo (2023); https://doi.org/10.5281/zenodo.7853649.

ACKNOWLEDGMENTS

We thank S. Aerts and J. Janssens for helping preprocess the data and for their constructive advice on annotation, N. Perrimon for suggestions during the initiation of this project, L. Buttitta for comments on polyploid phenotypes, and A. Parkhitko for discussion on metabolic pathways. We thank A.-L. Hsu (NYCU) for supporting C.-Y.L.; C. Desplan for supporting Y.-C.C.; and C. Qi, M. Burns, and all other lab members for comments and feedback during the project. We also thank the FCA Consortium and the fly community for their enthusiastic support. **Funding:** M.B. acknowledges the support of EPFL. T.J. was supported by Baylor College of Medicine Cancer and Cell Biology program grant T32 (GM136560). H.J.B. is supported by NIH/NIA (R01 AG07326), the Huffington foundation, and the endowment of the Chair of the Neurological Research Institute. L.L. is an investigator of the Howard Hughes Medical Institute and supported by NIH (R01-DC005982). L.L. and S.R.Q. are supported by Wu Tsai Neuroscience Institute (Neuro-omics program). This work was supported by CZ Biohub (S.R.Q.). S.L. was supported by a training award from NYSTEM contract C32559GG and the Center for Stem Cell Biology at MSKCC. Work in the E.C.L. group was supported by NIH/NINDS (R01-NS083833) and NIH MSK Core Grant P30-CA008748. Y.-C.C. was supported by the MacCracken Program at New York University, by a NYSTEM institutional training grant (contract C322560GG), and by a Scholarship to Study Abroad from the Ministry of Education, Taiwan. C.-Y.L. is supported by the NSTC grant from Taiwan (110-2311-B-A49A-501-MY3). H.L. is a CPRIT Scholar in Cancer Research (RR200063) and supported by NIH (R00AG062746), the Longevity Impetus Grant, the Welch Foundation, and the Ted Nash Long Life Foundation.

Author contributions: Conceptualization: T.-C.L., L.L., H.J., S.R.Q., and H.L. Sample preparation: N.S.K., X.T.C., and H.L. Sequencing: S.S.K., Y.Q., R.C.J., and H.L. Computational analysis: T.-C.L., M.B., J.L., T.J., and D.W. Data portal and AFCA website: J.C., T.-C.L., S.D., S.H.D., and A.O.P. APA analysis: S.L., Y.-C.C., and E.C.L. Data validation: Y.-J.P., H.J.B., T.J., Y.Q., N.A., and C.-Y.L. Writing: T.-C.L., M.B., and H.L. Review and editing: All authors. Supervision: H.J., S.R.Q., and H.L. Funding acquisition: H.J., S.R.Q., and H.L.
Competing interests: H.J., N.S.K., and X.T.C. are employees of Genentech, Inc. The other authors declare that they have no competing interests. **Data and materials availability:** All data are available for querying at https://hongjielilab.org/afca. Raw FASTQ files and processed h5ad files, including expression matrices and cell type annotations, can be downloaded from NCBI GEO under accession number GSE218661. Count matrices and analysis codes for generating the figures are available in Zenodo (*53*). FCA data were downloaded from https://www.flycellatlas.org/.

SUPPLEMENTARY MATERIALS

View/request a protocol for this paper from *Bio-protocol*.

Submitted 5 December 2022; accepted 4 May 2023
10.1126/science.adg0934

Aging Fly Cell Atlas identifies exhaustive aging features at cellular resolution

Tzu-Chiao Lu, Maria Brbi, Ye-Jin Park, Tyler Jackson, Jiaye Chen, Sai Saroja Kolluru, Yanyan Qi, Nadja Sandra Katheder, Xiaoyu Tracy Cai, Seungjae Lee, Yen-Chung Chen, Niccole Auld, Chung-Yi Liang, Sophia H. Ding, Doug Welsch, Samuel DSouza, Angela Oliveira Pisco, Robert C. Jones, Jure Leskovec, Eric C. Lai, Hugo J. Bellen, Liqun Luo, Heinrich Jasper, Stephen R. Quake, and Hongjie Li

Science, **380** (6650), eadg0934.
DOI: 10.1126/science.adg0934

Editor's summary
Aging is a fundamental process in multicellular life, and many phenotypes associated with aging are conserved across mammals and beyond. However, characterizing cellular processes across tissues over the life of an organism has been historically difficult to achieve. Lu *et al*. performed single-nucleus RNA sequencing at multiple time points across the life span of the fruit fly, *Drosophila melanogaster*. After examining more than 850,000 nuclei across 163 cell types, the authors identified changes in gene expression and cellular composition during the aging process and used them to develop an aging clock. This atlas will serve as a resource for studying the process of aging in this important model organism. —Corinne Simonti